EXPERIMENTAL INVESTIGATION OF A SOLAR LiCl DRYER SYSTEM

Elias Yazdanshenas
Azad University of Semnan Branch
Semnan _ Damghan Road, Semnan, Iran
elias_yazdanshenas@yahoo.com

Faezeh Asgari
Mazandaran Institue of Technology
Babol Mazandaran, Iran
f_asgari45@yahoo.com

Eshagh Yazdanshenas
Ebert & Baumann Consulting Engineers,
Washington D.C.
E.yazdanshenas@eb-engineers.com

ABSTRACT

Solar LiCl air dryer system has been investigated theoretically and experimentally. It consists of three parts: the main dryer part with liquid desiccant solution (LiCl) cycle, the solar heating system with sensible and latent heat stores, and the ground source.

The dryer system includes dehumidifier to decrease air humidity and the regeneration section that was designed to increase the concentration of LiCl solution. For the experiments, the supply heat energy in the heat storage tank was an electrical heater that provides the required energy similar to the solar heating system with PCM material investigated by the author (1). Also, cold water was used for the experiments instead of the ground source for cooling the LiCl solution in the heat exchanger before entering the dehumidifier.

In this paper, the experimental results will be presented. The theory of the experimental setup with the solar heating system with PCM material and the ground source is investigated.

Keywords: Solar energy, Phase Change material (PCM) tank, Liquid desiccant solution (LiCl) Ground source.

1. INSTRUCTION

Air conditioning systems consume a considerable amount of energy. Renewable energy like solar energy would be a good choice to be used in the thermodynamic cycle. Crofoot and Harisson (2), Andrusiak, Harrison, (3) considered using solar air conditioning systems.

The main part of the whole cycle is the dryer part and also choosing the working fluid in the dryer cycle.

According to Liu et al. (4) finding, in the dehumidification process, LiCl compared to LiBr in the same condition (the same vapor pressure and inlet temperature, rather than the same crystal temperature) had a better mass transfer performance in the same desiccant mass flow rate condition. they reported that the COP of using Licl and LiBr in the cycle is similar. Additionally, initial cost of LiCl solution price is 18% lower than LiBr.

Khan and Martinze (5) developed a simple model to predict the performance of liquid desiccant absorber. They showed that the simple model had a good agreement with the detailed model.

Phase Change Material tanks have been used extensively in various literature. Ismail (7) investigated a numerical model to simulate a latent storage tank composed of spherical capsules filled with PCM placed inside a cylindrical tank filled with a working fluid circulation system to charge and discharge energy in the heat storage tank. The influence of charging and discharging time of the PCM tank were investigated numerically and experimentally. Water Heating System was also improved with the use of Phase Change Materials (8-9).

Ground source can be used for cooling the working fluid temperature. Bernardi at el. (10) investigated that it is useful to improve a cycle and increasing COP of whole cycle by using ground source.

In the current paper LiCl dryer has been investigated experimentally and theoretically combined with solar heating system with PCM tank and also ground source cycle.

2. Experimental Investigation

1. Governing equation

1.1. Dehumidifier and Regeneration

According to Liu at el. (4) paper, the equivalent humidity ratio of liquid desiccant ω_e is illustrated with the equilibrium status of air, as shown in Eq. (1),

ωe=0.622PsB-Ps
Eq. 1

Moisture removal rate in the mass transfer performance of the dehumidifier or regenerator is shown in Eq. (2).

mw=ma.ωa,in-ωa,out
Eq. (2)

Eq. (3) expresses the relation of moisture removal rate in the dehumidifier. Additionally, the regressed moisture removal rates using LiCl are shown in Eq. (4). Meanwhile, in Eq. (5), the volumetric mass transfer coefficient is illustrated.

mwLiCl, dehum=9.4542×108×ma0.406. ωa2.2478 .ms,in0.6499. ts,in -2.3911.ξin1.7919 Eq. 3

mwLiCl, regen=6.602×10-8×ma0.1649. ωa-0.4617 .ms,in0.4818. ts,in 3.223.ξin-2.9341
Eq. 4

hmaLiCl, regen=4.6645×νa0.6562×νs0.5694× ϕe,in-0.2280 Eq. 5

In the regeneration or dehumidifier, on the analytical solution of the heat and mass transfer procedure in packed-bed, the mass transfer efficiency εm at diverse flow patterns is the function of heat capacity ratio of air to desiccant m*and mass transfer unit NTU_m, as shown in Eq. (6), Eq. (7) and Eq. (8) investigated in (4) and (11-12).

εm=ωa,in-ωa,outωa,in-ωe,in=fm*,NTUm
Eq.6

m*=Cp.e . maCp,s . ms=Cp.e . ρa . VaCp,s . ρs . Vs Eq. 7

where Cp,e= dhedts

NTUm=hmma=hma .Vma
Eq. 8

The higher mass transfer efficiency is brought the moisture removal rate as shown in Eq. (9).

mw=εm . ma.ωa,in-ωe,in
Eq. 9

Eq. (10) infers that the coefficient of performance of the liquid desiccant system is determined by the cooling capacity of the processed air Q_a divided by the regeneration heat supplied into the regenerator Q_{hot}.

COP=QaQhot= ma .(ha,in- ha,out)Cp,wh . mwh .(twh,in- twh, out)
Eq.10

1.2. Solar thermal system

In the following equations, the solar collector efficiency and PCM tank efficiency are shown.

1) Solar collector: In the Eq. (13), solar collector efficiency is calculated where the solar collector heat transfer rate is calculated in Eq. (12).

Qu=mccwTic-Toc
Eq.(12)

ηc=QuAcGc Eq.13

2) PCM tank: For PCM tank efficiency shown in Eq. (16), PCM heat transfer rate (Eq. (14)) was divided by the maximum possible heat transfer rate that the PCM tank is able to save. In addition, data logger receives experimental data every 30 minutes. Therefore Eq. (15) needs to be divided by the period of 30 minutes in order to convert it to kW.

Qs=mtcwTit-Tot
Eq.14

Qp=mpcmcpcmTpcm-Ta
Eq.15

ηt=30×60QsQp
Eq. 16

2.1.2 Ground source temperature estimation

According to previous research investigation (13), T_g is the undisturbed ground temperature expressed in °k. It can be calculated as:

TgXs, t=Tg-Asexp-Xsπ365α

cos2π365t-t0-Xs2365π α-321.8+ 273

Eq. 17

where X_s, t, $\overline{T}_g$, A_s, α and t_o are the soil depth in feet, the day of year, annual surface soil temperature, the annual surface temperature amplitude (T_{max}-T_{min}), the soil thermal diffusivity[1], and a phase constant expressed in days, respectively. Eqs. (18-19) are the minimum and maximum ground temperatures for any depth, respectively.

Tg,min= Tg- As exp-Xsπ365α
Eq.18

Tg,max= Tg+As exp-Xsπ365α
Eq. 19

According to Kavanaugh et al. (14), for vertical ground source systems, X_s can be fixed equal to the average depth in Eq. (18) and Eq. (19). Temperature can be estimated approximately as equal to the mean annual surface soil temperature, $\overline{T}_g$.

1 α = k / ρ C_p where k is the thermal conductivity in BTU/ hr lb °F, ρ is the density in lb / ft^3 and C_p is the spicific heat in BTU/ lb °F.

For calculating ground heat exchanger length Eq. (20) in the Ground Source Heat Pump (GSHP) Project, Model of International Ground Source Heat Pump Association (IGSHPA) (13) is utilized as the method. The required Ground Heat Exchanger (GHX) length L_c establish on cooling necessity:

Lc= qd ,coolCOPc+1COPcRp+RsFcTewt, max-Tg, max Eq. 20

Where COP_c is the design cooling coefficient of performance (COP) of the heat pump system, F_c is the part load factor for cooling, R_s is the soil thermal resistance, R_p is the pipe thermal resistance, T_{gmax} , is the maximum undisturbed ground temperature, and $T_{ewt,max}$ is the maximum design entering water temperature at the heat pump.

The method that the model used in the Natural Resources Canada (RETScreen) GSHP Project Model used to model the COP and the capacity as a function of the entering fluid temperature uses a quadratic polynomial correlation:

COPactual=COPbaseline K0+K1Tewt+K2Tewt2 Eq. (21)

K0= 1.53105836
K1=-2.29609500×10^{-2}
K2=6.87440000×10^{-5}

Where COP_{actual} is the actual COP of the heat pump, $COP_{baseline}$ is the nominal COP of the heat pump (e.g. measured at standard rating conditions, 0°C for heating and 25°C for cooling), k_i are correlation coefficients listed and Q_c is the capacity of the heat pump for cooling or heating.

The maximum and minimum design temperature of entering water are pinted out in Eqs. (22, 23) :

Tewt,min=Tg,min-15oF-321.8
Eq. 22

Tewt,max=min(Tg,max+20oF ,110oF)-32/1.8

Eq.23

Because the model was also designed to be used in permafrost, the 20°F minimum entering water temperature limitation was not implemented.

The part load factor (F) is calculated by divided the full load hours during the design month by the total number of hours in that month, as seen by the GHX Eq. (24). It can be evaluated as:

$$F = \frac{q}{q_{max}} \qquad \text{Eq. 24}$$

Where q_{max} and q are the peak load for the month and the average load respectively.

3. Method

In the dryer cycle, LiCl as the working fluid circulated in the dehumidifier to absorb air humidity. To have LiCl with high concentration, regeneration part is designed in the dryer cycle. Heat resource is provided by electrical heater. Later, instead of the electric heater, solar collectors and PCM tank were used theoretically. Fig. 1 shows a schematic diagram of the LiCl dryer with solar heating system which consists of 3 parts:

1. Solar collector and heat storage tank:

During the day, the solar collectors are exposed to the solar radiation and thus produce hot water. Hot water is divided between the heat storage tank (HST) and PCM tank (Fig. 2). Heat storage tank is a heat exchanger that transfers the heat energy from solar collectors to dryer cycle. Additionally, dryer cycle does not need constant heat energy because sometimes the percentage of concentration of the solution is enough not to regenerate.

During day, solar collectors produce heat energy in the PCM tank and can be discharged during night in dryer cycle when it is demanded. Additionally, thermo physical properties of the PCM are shown in TABLE. 1.

TABLE. 1: THERMO PHYSICAL PROPERTIES OF THE PCM (PARAFFIN).

Melting point	55-59°c
Heat storage capacity	178 (Kj/kg)
Solid Density	900 (m3/kg)
Liquid Density	770(m3/kg
Thermal conductivity	2. (W/m.K)

3.

2. Drying system with LiCl working fluid:

4.

5. Whole dryer system is shown in Fig. 3. where in the dehumidifier part, LiCl solution splashes on the cellulose pad and a fan blows ambient air on the cellulose pad guided by the duct channel. Therefore, dried air leaves the pad outlet to be used in air conditioning system. In the regeneration part, Heat Storage Tank (HST tank) is applied between the solar collector and regeneration part of the dryer cycle. It should be mentioned that when LiCl concentration decreases, valves number 12, 19 will be closed and valves 13, 18 are opened to regenerate in the regeneration). The hot LiCl solution (valve 13) enters the cellulose pad and splashes on it by the Pump to create high LiCl concentration. When the system has enough LiCl concentration, valves 12 and 19 are opened and valves 13 and 18 are closed until the LiCl concentration becomes low. The LiCl concentration is controlled manually by measuring the LiCl and opening and closing the valves.

6.

7. 8.

9.

10. Fig. 2: HST and PCM tank.

11.

12.

13. Fig. 3: Dryer system with Liquid desiccant LiCl.

14.

15.

16.

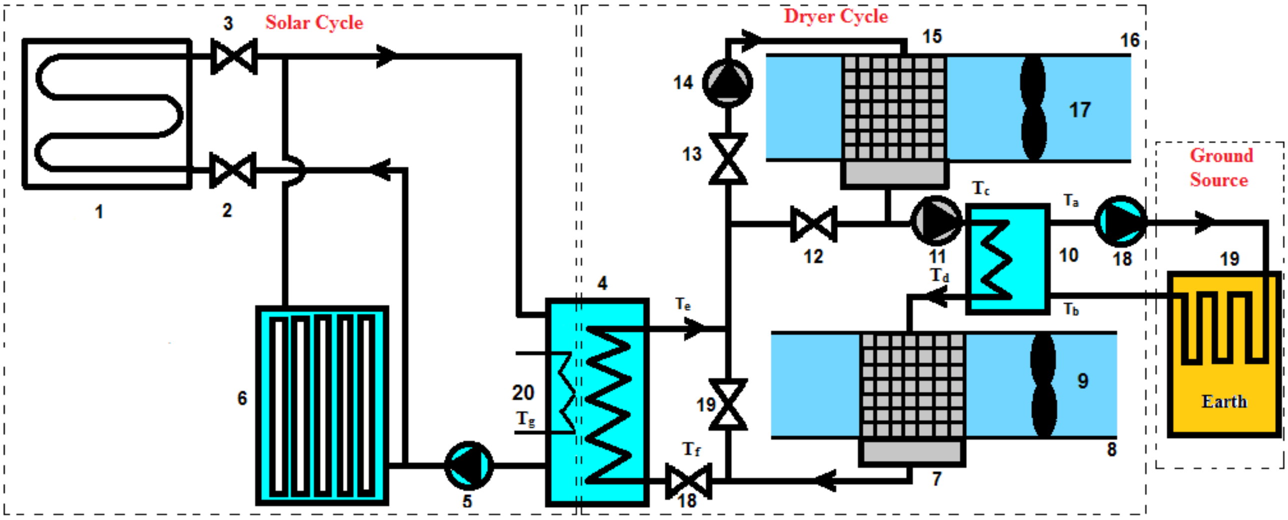

17. Number	18. Name	19.	20. Number	21. Name
22. 1	23. Collector	24.	25. 8, 16	26. Air Channel
27. 2, 3,	28. Valve	29.	30. 9	31. Fan

12, 13,18,19			, 17	
32. 4	33. Heat storage tank (HST)	34.	35. 10	36. Heat exchanger B
37. 5, 11, 14,18	38. Pump	39.	40. 19	41. Ground Source
42. 6	43. PCM tank	44.	45. 20	46. Electrical Heater
47. 7, 15	48. Cellulose pad	49.	50.	51.

52. Fig. 1: Whole solar dryer cycle with use of ground source.

53.

54. TABLE 2: LICL PROPERTIES.

55. Air		56. LiCl solution		57. Wa	58. Fluid
59. 30	60. 70	61. 30	62. 70	63. 20	64. Temperature (°C)
65. 1.8	66. 0.998	67. 1260	68. 126	69. 100	70. Density (kg/m^3)
71. 1.0058	72. 1.009	73. 2.7	74. 2.8	75. 4.1	76. Specific heat (KJ/kg ◦C)
77. 1.746×10^{-5}	78. 2.07×10^{-5}	79. 3.5×10^{-3}	80. 2.5×10^{-3}	81. 10.006×10^{-5}	82. Viscosity(Pa.Sec)

83. 0.026	84. 0.03	85. 0.55	86. 0.8	87. 0.5	88. Thermal Conductivity 89. (W/m.K)
90. 0.708	91. 0.697	92. -	93. -	94. 7.0	95. Prandtl Number

96.

97.

3. <u>Using Geo source for cooling LiCl solution.</u>

98.

99. If LiCl liquid desiccant temperature decreases, it can absorb much more humidity, therefore, ground source system which has water as a working fluid is used. It can be used in the heat exchanger B in the dryer cycle. The dryer system would be effective because it does not need to have cooling tower in the cycle especially when the cycle is in the humid climate. Finally, LiCl solution with high concentration comes back in dehumidifier part after heat exchanger B outlet and it can absorb the air humidity.

100.

101.

102.

103.

104.

105.

106. 107.

108. Fig. 4: Cellulose pad and the heat exchangers used in LiCl dryer system.

4. <u>Experimental test</u>

109.

110. Humidity, temperature and air velocity in LiCl dryer are measured by SAMWON model SU-50313, model TESLINK RS-232 and Model Smart Sensor AR846 respectively.

111.

112. The solar thermal system had different setup located in a different location. Solar system was set up in the latitude of 35.39, longitude of 53.2 and altitude of 1127.29m. In this experimental work, solar radiation is measured using Kipp & Zonen pyranometer. The data logger has LM35 temperature sensors with the temperature accuracy of ±0.1°c.

113.

5. <u>Results and Discussion</u>

114.

115. The desired air mass flow rate assumed to be 0.54 kg/s and according to Eqs. (3) and (4), the LiCl

solution flow rate in the dryer cycle is calculated to be 0.23 kg/s depending on the moisture removal and also moisture content created by dryer the cycle. The parameters measured in this experiment are inlet and outlet temperature, humidity and flow rates both in the air side, water side and LiCl solution side. Table 3 shows the measured data. The result shows that the ambient air humidity can be decreased well from 66% and temperature of 32°C down to 30% of humidity with 35°C of the delivered air. There is no significant change in the air temperature.

116.

117. TABLE 3. DATA OF Whole LiCl DRYER AT SAME TIME

118. Ambient air temperature	119. 32°
120. Ambient air humidity	121. 66
122. Outlet air temperature in dehumidifier	123. 32.
124. Outlet air humidity in dehumidifier	125. 30
126. Humidity air	127. 66
128. Flow of inside air the humidifier and Regeneration part	129. 0.5
130. Outlet humidity air in regeneration	131. 80
132. Outlet temperature air in regeneration	133. 35°
134. LiCl solution flow	135. 0.2
136. Inlet water heat exchanger B(T_b)	137. 18°
138. Outlet water heat exchanger B(T_a)	139. 29°
140. Water in heat exchanger B	141. 0.1
142. Inlet LiCl solution heat exchanger B(T_c)	143. 50°
144. Outlet LiCl solution heat exchanger B(T_d)	145. 41°
146. Inlet Licl heat storage tank(T_f)	147. 40°
148. Outlet Licl heat storage tank (T_g)	149. 52
150. Average water temperature inside heat storage tank	151. 58

152.

153. According to Table 3, the measured heat storage tank temperature with water was measured to be 58°C. The current heat storage tank had an electric heater. However, solar thermal system can be used to provide the required temperature. Auxiliary supply system with electric heater can still be connected to the system.

However, less energy can used to heat up and keep the heat storage tank constant. Therefore, solar thermal system with PCM material is introduced to the system. According to Fig. 5, solar radiation, inlet and outlet temperature of solar collector are shown in a specific sunny day.

154.

155. The inlet and outlet solar collector temperatures are changed with delay because of absorbing energy by PCM tank material that release the heat smoothly to the water tank heat store in order to stabilize the temperature.

156.

157.

158. Fig. 5: Inlet and outlet temperatures from the solar collector (to the left), solar radiation (to the right).

159.

160.

161. Fig. 6: Heat storage tank temperature versus the time (hr).

162. The minimum temperature for heat exchanger B inlet temperature in the LiCl dryer cycle is 18°C. Fig.7 illustrates typical soil temperature variation reported by Kavanaugh and Rafferty (14). If the depth of the hole is higher, the soil temperature will decrease and finally become constant at 6°C. Therefore, ground source can be used in the heat exchanger B side in order to provide temperature less than 18°C. Ground source can be used especially in the humid climate where instead of the cooling tower, ground source can be used.

163.

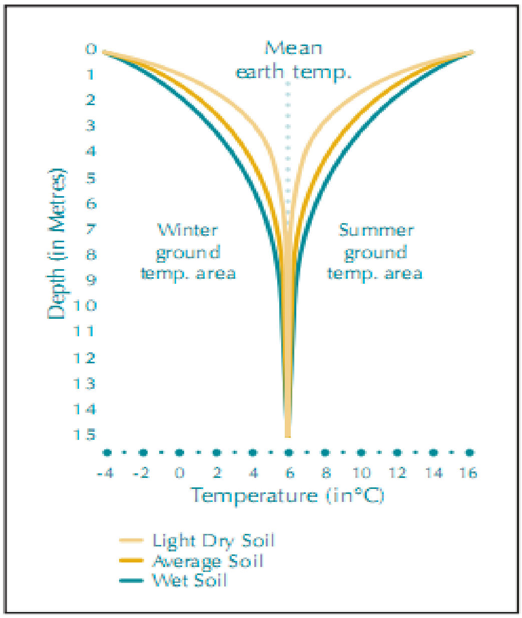

164. Fig 7: Typical soil temperature variation (14).

165.____

6. Conclusion

166.____

167. Dryer system with LiCl solution as a working fluid can was investigated experimentally. The system showed that the dry ambient air with 0.54 kg/s from 66% to 30%.

168. The experimental investigation was carried out to test the PCM tank heat storage and water heat storage tank in order to use them for regeneration of the LiCl solution. The PCM tank can store solar energy during day and can deliver heat to the water heat storage tank for longer time during night, especially when the regeneration part is used in the dryer cycle during evening and night.

169.

170. In humid climate, it is difficult to benefit from cooling tower in the dryer cycle. Therefore ground source can be used in the dehumidification process.

171.

172.

173.

7. Nomenclature

174.

175.

176. 177.

178.	A	179.	Mass transfer area, m^2	180.	C_{PCM}	181.	PCM Specific heat, kJ/(kg°k)
182.	a	183.	Specific area of the packing per volume, m^2/m^3	184.	T_{pcm}	185.	Melting temperature PCM, k
186.	B	187.	Atmospheric pressure, Pa	188.	T_a	189.	Air temperature, °k
190.	C_p	191.	Specific heat capacity, kJ/(kg°k)	192.	η_t	193.	PCM tank efficiency
194.	H	195.	Enthalpy, kJ/kg	196.	T_g	197. 198. 199.	ound mperature
200.	COP	201.	Coefficient of performance of the liquid desiccant system,	202.	X_s	203.	Soil depth, m
204.	h_m	205.	Convective mass transfer coefficient, kg/(m^{2}s)	206.	T	207.	The day of year, k
208.	h_{ma}	209.	Volumetric mass transfer coefficient, kg/(m^{3}s)	210.	$\bar{T}_g$	211.	Annual surface soil temperature, k
212.	N	213.	Superficial velocity, m/s	214.	A_s	215.	The annual surface temperature, k amplitude (Tmax-Tmin), m^2

216.	ε_m	217.	Mass transfer efficiency, %	218.	A	219.	Soil thermal diffusivity
220.	Φ	221.	Relative humidity, %	222.	t_o	223.	Phase constant expressed in days
224.	Ω	225.	Humidity ratio, kg/kg	226.	Tg,min	227.	Minimum ground temperature, k
228.	m	229.	Mass flow rate, kg/s	230.	Tg,max	231.	Maximum ground temperature, k
232.	m*	233.	Heat capacity ratio of air to desiccant, dimensionless	234.	Lc	235.	Ground heat exchanger length
236.	m_w	237.	Moisture removal rate, kg/s	238.	COP_h 239.	240.	design cooling coefficient of performance (COP) of the heat pump system
241.	NTU_m	242.	Mass transfer unit, dimensionless	243.	Fc	244.	part load factor for cooling
245.	P	246.	Vapor pressure, Pa	247.	R_s	248.	soil thermal resistance
249.	Q	250.	Cooling capacity or heating capacity, kw	251.	R_p	252.	pipe thermal resistance
253.	t	254.	Temperature, ℃	255.	T_{gmax}	256.	the maximum undisturbed ground temperature, k
257.	v	258.	Volume of the packed-bed module, m^3	259.	$T_{ewt,max}$	260.	maximum design entering water temperature at the heat pump
261.	ξ	262.	Mass concentration	263.	COP_{actual}	264.	the actual COP

	of liquid desiccant (solute/solution), %		of the heat pump
265. ρ	266. Density, kg/m^3	267. $COP_{baseline}$	268. ominal COP of the heat pump
269. Q_u	270. Collector Heat transfer rate, w	271. $T_{ewt,min}$	272. inimum design entering water temperature
273.	275.	277.	279.
274. m_c	276. Mass flow rate of collector, kg s^{-1}	278. $T_{ewt,max}$	280. aximum design entering water °k temperature
281. T_{ic}	282. Collector Inlet temperature, k	283. F	284. art load factor
285. T_{oc}	286. Collector Outlet temperature, k	287. q_{max}	288. eak load for the month
289. η_c	290. Collector Efficiency	291. q	292. verage load,

293. A_c	294. Collector Area, m^2		
295. G_c	296. Solar radiation, W m^{-2}	297. A	298. Humid air
299. Q_s	300. PCM Storage tank Heat transfer rate, w	301. In	302. Inlet
303. m_t	304. Mass Flow rate PCM tank, kg s-1	305. out	306. Outlet
307. T_{it}	308. PCM tank inlet temperature, k	309. S	310. Liquid desiccant
311. T_{ot}	312. PCM tank Outlet temperature, k	313. W_h	314. Hot water
315. Q_p	316. Max Heat PCM Storage tank, J	317. ω_e	318. humidity ratio of liquid desiccant
319. m_{pcm}	320. PCM mass, Kg	321.	322.

323.

8. References

324.

325. (1) Elias Yazdanshenas and A. Khalesi doost, Energy saving of a solar heating system with Phase Change Material (PCM) heat exchanger: Solar World Congress, 2011

326. (2) Lisa Crofoot and Stephon Harisson, Evaluation of a liquid desiccant air conditioning system with solar thermal regeneration: Solar World congress, 2011

327. (3) Andrusiak, M., Harrison, S.J., The modeling and design of a solar-driven liquid desiccant air-conditioning system: Canadian Solar Building Research Network /Solar Energy Society of Canada Conference, Toronto ON, 2009

328. (4) X.H. Liu, X. Q. Yi, Y. Jiang, mass transfer performance comparison of tow commonly used liquid desiccants: LiCl and LiBr aqueous solution:

Energy Conversion and Management - ENERG CONV MANAGE , vol. 52, no. 1, pp. 180-190, 2011

329. (5) Khan A. Y. and Martinze J. Modeling and parametric analysis of heat and mass transfer performance of a hybride liquid dessicant absorber: Energy converse. Manage, 39(10), 1059-1112, 1998

330. (7) K.A.R. Ismail, J.R. Henriquez, Numerical and experimental study of spherical capsules packed bed latent heat storage system: Applied Thermal Engineering 22 1705–1716, 2002

331. (8) Vikram D, Kaushik S, Prashanth V, Nallusamy N" An Improvement in the Solar Water Heating Systems using Phase Change Materials: Proceeding of International Conference on Renewable energy For developing countries, 2006

332. (9) Velraj, R. and Seeniraj, R.V., Heat transfer studies during solidification of PCM inside an internally finned tube: Journal of Heat Transfer, 121: 493-497, 1999

333. (10) BernardiWP, Blevins RP, Sloane BD. Examination and life assessment of field-ested heat pump water heaters: Prepared by Energy Utilization Systems, incorporated for Oak Ridge National Laboratory operated by Union Carbide Corporation for the U.S. Department of Energy, 1982

334. (11) Liu XH, Jiang Y, Xia JJ, Chang XM. Analytical solutions of coupled heat and mass transfer processes in liquid desiccant air dehumidifier/regenerator: Energy Converse Manage;48(7):2221–32, 2007.

335. (12) Ren CQ, Jiang Y, Zhang YP. Simplified analysis of coupled heat and mass transfer processes in packed bed liquid desiccant-air contact system: Solar Energy; 80 (1):121–31, 2006.

336. (13) IGSHPA, Closed-Loop/Ground-Source Heat Pump Systems – Installation Guide: International Ground-source Heat Pump Association, Oklahoma State University, Stillwater, Oklahoma, USA, 1988

337. (14) Kavanaugh, P.K. and Rafferty, K., Ground-source Heat Pumps – Design of Geothermal Systems For Commercial and Institutional Buildings: American Society of Heating, Refrigerating and Air-Conditioning Engineers, Inc., 1791 Tullie Circle, N.E., Atlanta, GA, USA, 1997

338.